122 J. Med. Chem. 2011, 54, 122–130
DOI: 10.1021/jm100860s

Journal of Medicinal Chemistry Article

Ursodeoxycholic Acid Amides As Novel Glucocorticoid Receptor Modulators

Ruchika Sharma,*[,†,‡] David Prichard,[‡] Ferenc Majer,[†] Anne-Marie Byrne,[‡] Dermot Kelleher,[‡] Aideen Long,[‡] and John F. Gilmer*[,†]

[†]*School of Pharmacy and Pharmaceutical Sciences, Trinity College Dublin, Dublin 2, Ireland, and* [‡]*Cell Signalling, Institute of Molecular Medicine, Trinity Centre for Health Science, St. James's Hospital, Dublin 8, Ireland*

Received July 9, 2010

Ursodeoxycholic acid (UDCA) is used for the treatment of hepatic inflammatory diseases. Recent studies have shown that UDCA's biological effects are partly glucocorticoid receptor (GR) mediated. UDCA derivatives were synthesized and screened for ability to induce GR translocation in a high content analysis assay using the esophageal cancer SKGT-4 cell line. UDCA derivatives induced GR translocation in a time dependent manner with equal efficacy to that of dexamethasone (Dex) and with greatly increased potency relative to UDCA. The cyclopropylamide **1a** suppressed TNF-α induced NF-κB activity and it induced GRE transactivation. **1a** was unable to displace Dex from the GR ligand binding domain (LBD) in a competition experiment but was capable of coactivator recruitment in a time-resolved fluorescence energy transfer assay (TR-FRET). This represents a novel mechanism of action for a GR modulator. These derivatives could result in a new class of GR modulators.

Introduction

The glucocorticoid receptor (GR[a]) is a member of the nuclear receptor family of eukaryotic transcription regulators.[1] Classical GR agonists (glucocorticoids, GCs) include the endogenous GR ligand cortisol and its synthetic derivatives. GCs are the principal therapies in asthma, rheumatoid arthritis, and inflammatory bowel disease.[2] They also find clinical application in neurological conditions and in certain types of cancer.[3] The GR is arguably the most important pharmacological target in medicine.

The unliganded GR resides in the cytoplasm, part of a multimeric complex consisting of the GR polypeptide and chaperone proteins hsp90 and immunophilins, FKBP52, FKBP51, Cyp40, and PP5.[4] Ligand binding causes dissociation of chaperones leading to exposure of nuclear localization signals triggering nuclear translocation. Ligand-bound GR may dimerize. Homodimeric GR has direct and indirect effects on a wide spectrum of transcriptional activities.[5] Binding to glucocorticoid response elements (GREs) followed by coactivator recruitment results in transactivation of genes.[6−9] Homodimers can also bind to negative GREs, inhibiting gene expression.[10,11] Yet another pathway involves direct binding to pro-inflammatory transcription factors such as activator protein-1 (AP-1) and nuclear factor κ-light-chain-enhancer of activated B cells (NF-κB).[5,12] This "transrepression" effect is associated with GR monomers.[13] There has been in the past few years an interest in so-called "dissociated steroids" that can separate transrepression from transactivation, which is associated with steroid side effects.[14−17] Steroid antagonists also cause receptor dissociation and nuclear translocation but with limited transcription. GC antagonists are being investigated in a range of indications including, psychotic depression, diabetes, obesity, Alzheimer's disease, neuropathic pain, drug abuse, and glaucoma.[18] Thus it is possible to envisage ligands capable of inducing GR translocation but associated with a more limited repertoire of transcriptional activities than classical GC agonist. Mechanistically, such compounds should bind nonclassically, influencing GR self-association and recruitment of transcriptional machinery.[19]

UDCA (UDCA, **1**, Figure 1), a traditional medicine, is used at high dose in the treatment of primary biliary cirrhosis (PBC) and primary sclerosing cholangitis.[20] The biochemical basis for UDCA's actions remains somewhat obscure although it is the subject of extensive investigation. UDCA exhibits antiapoptotic action in hepatic[21,22] and nonhepatic cell lines,[23,24] and it has neuroprotective actions.[25−27] It has putative chemopreventative effects in colon cance,r[28] and it has been shown to attenuate carcinogenic signaling cascades induced by other bile acids. These include inhibition of protein kinase C translocation,[29] suppression of p38, MAPK, and Cox-2 expression[30] as well as reduction in activity of the transcription factors AP-1 and NF-κB.[31] UDCA treatment reduces serum antimitochondrial and immunoglobulin G antibodies.[32] It can also suppress interleukin-2[33] and interferon γ production[34] and decrease the hepatocellular and

*To whom correspondence should be addressed. For R.S.: phone, +35318963350/8962844; fax, +35318962810; E-mail, rsharma@tcd.ie. For J.F.G.: phone, +35318962795; fax, +35318962793; E-mail, gilmerjf@tcd.ie.

[a] Abbreviations: AP-1, activator protein-1; CDCA, chenodeoxycholic acid; DCA, deoxycholic acid; Dex, dexamethasone; GCs, glucocorticoids; GR, glucocorticoid receptor; GREs, glucocorticoid response elements; HRMS, high resolution mass spectrometry; HPLC, high performance liquid chromatography; HCl, hydrochloric acid; LBD, ligand binding domain; LPS, lipopolysaccharide; $MgSO_4$, magnesium sulfate; MeOH, methanol; NF-κB, nuclear factor κ-light-chain-enhancer of activated B cells; PBS, phosphate buffered saline; PLA_2IIA, phospholipase A_2 IIA; PBC, primary biliary cirrhosis; PSC, primary sclerosing cholangitis; TR-FRET, time-resolved fluorescence energy transfer; SRC1−4, steroid receptor coactivator 1−4; TLC, thin layer chromatography; TAT, tyrosine aminotransferase; UDCA, ursodeoxycholic acid.

 Published on Web 12/15/2010

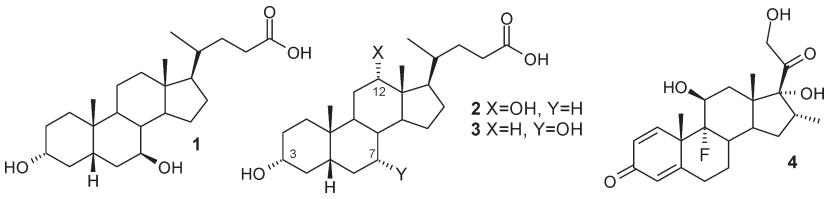

Figure 1. Structural formulas of UDCA (**1**), DCA (**2**), CDCA (**3**), and Dex (**4**).

Scheme 1. Synthesis and Structural Formulas of UDCA analogues **1a**−**1k**

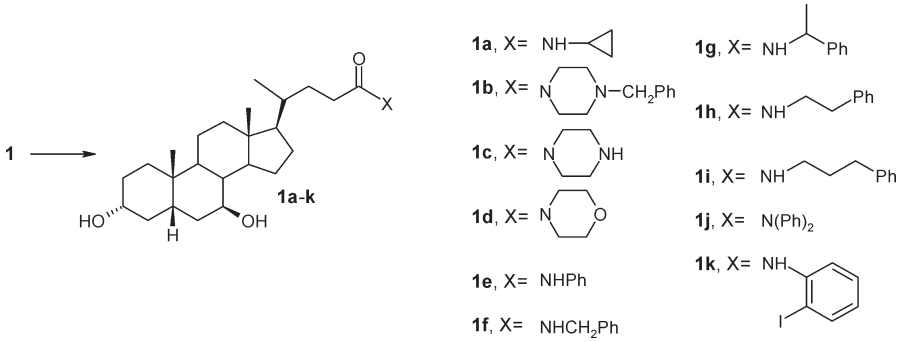

(i) Formic acid/perchloric acid, 47 °C, 3 h; (ii) $SOCl_2$, reflux, 2 h; (iii) RNH_2, NEt_3, RT; (iv) NaOMe/MeOH, 70 °C, 2 h.

biliary expression of both major histocompatibility complex class I and class II molecules in patients with PBC.[35,36] UDCA can correct the defective natural killer cell activity by inhibiting prostaglandin E_2 production in PBC patients.[37] UDCA has a suppressive effect at the transcriptional level on phospholipase A_2 IIA (PLA_2IIA) in hepatocytes.

These latter effects at a physiological and biochemical level are similar to those of GCs.[38] There is also a significant body of biochemical evidence that UDCA can activate GR pathways. UDCA has been reported to induce translocation of the GR and to activate the GR in various different cell models.[39−42] Furthermore, UDCA can suppress NF-κB activity via activation of the GR.[41] The GR-ligand binding domain (LBD) is responsible for UDCA-dependent nuclear translocation of the GR.[41] GR knockdown attenuates UDCA's inhibitory effects on PLA_2IIA.[38]

Taking these studies and UDCA's clinical history of minimal side effects into account, we decided that it would make an excellent lead for the development of a novel class of GR modulators.

In this work, a series of bile acid derivatives (Scheme 1) were synthesized in order to test this hypothesis. Chronic inflammation in the esophagus has been associated with the pathogenesis of esophageal adenocarcinoma.[43] Hence we screened our derivatives for the ability to modulate the GR in an esophageal cancer cell line. We have shown that modification at the C24-position of UDCA leads to compounds endowed with the ability to induce GR translocation in the low micromolar range. These may act as leads for development of GR modulators with new transcriptional profiles. The increased potency of these analogues makes them useful tools for further characterizing UDCA's effects on the GR and elucidating its mechanism of action.

Results and Discussion

We initially established the ability of UDCA to induce translocation of the GR from the cytoplasm to the nucleus in the esophageal SKGT-4 cell line. UDCA weakly induced translocation of the GR from the cytoplasm to the nucleus (54% efficacy of Dex 100 nM (**4**) at 300 μM (Figure 2A−C). This is a similar level of effect to that reported in other cell lines. UDCA has three readily manipulable functional groups: the C3-, C7-OH, and C24-COOH (Figure 1). UDCA's ability to induce GR trafficking is connected with its C7-β OH group because its C7-epimer chenodeoxycholic acid (CDCA, **3**) and deoxycholic acid (DCA, **2**) do not induce GR trafficking. Our initial chemistry therefore focused on manipulating the C24-COOH group. This strategy was supported by the observation that TauroUDCA (TUDCA) can induce GR and mineralocorticoid receptor (MR) translocation, illustrating that the side chain could be modified and that amide derivatives of UDCA might be active.[44,45] We therefore targeted a small chemically diverse library of UDCA amides (**1a**−**k**, Scheme 1). These were produced in four steps from UDCA by formyl protection of the steroidal −OH groups, formation of the corresponding acyl chloride ($SOCl_2$), amidation with the appropriate amine, and deformylation (NaOMe/MeOH).

We produced another set of UDCA derivatives (**1l**−**1s**, Figure 3) in which the acid group was abolished or migrated using classical bile acid chemistry.[46,47]

Analogues **1a**−**1s** were tested in a high content analysis assay using immunofluorescence to estimate the nuclear to cytoplasmic ratio (Figure 4). The experiment was carried out initially at 300 μM for 4 h and repeated at successively lower concentration where an effect was observed (Table 1). The amide series (**1a**−**1k**) exhibited the highest biochemical efficacy relative to Dex and highest potency. For example, the cyclopropyl derivative (**1a**) and **1b**, **1c**, and **1d** had similar efficacy to Dex as reflected in steady-state nuclear/cytoplasmic ratio. **1a**−**b** were the most potent compounds with EC_{50} values of 7.3 and 5.6 μM, respectively (Figure 2D). Removal of the benzyl group in **1c** maintained GR translocation efficacy but reduced potency by 10-fold (50.8 μM). The anilide (**1e**) did not induce translocation but the benzylamide (**1f**), α-methylbenzylamide (**1g**) and phenethylamide (**1h**) showed

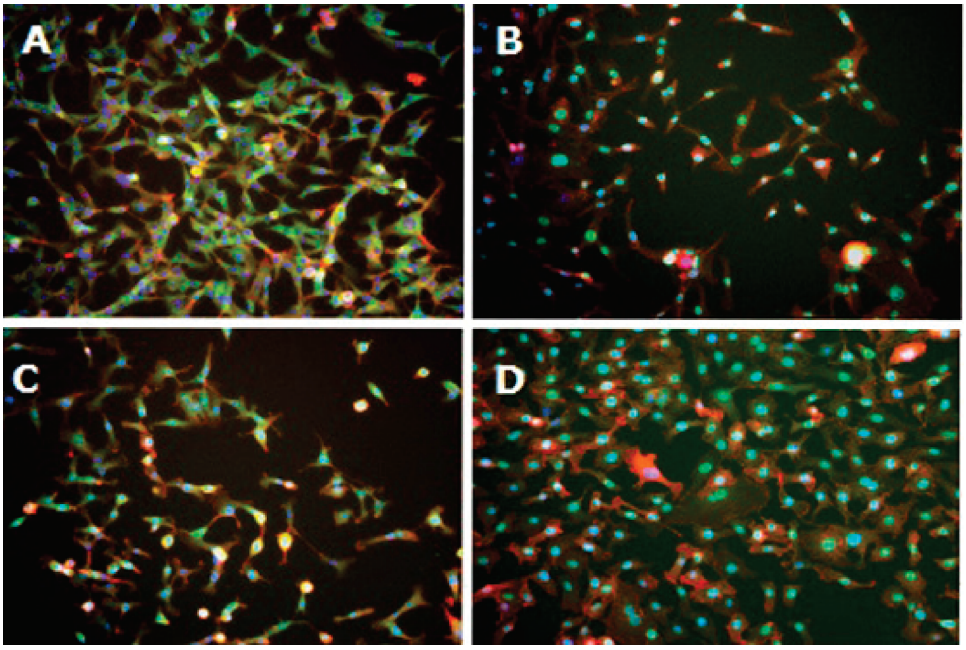

Figure 2. UDCA derivatives induce GR translocation. SKGT-4 cells were treated with (A) DMSO 1%, (B) Dex (100 nM) as a positive control, (C) UDCA (300 μM), or (D) **1a** (100 μM). Cells were fixed with paraformaldehyde 4% in PBS after 4 h. The GR was identified using a mouse monoclonal GR antibody (green.) and cells were stained with Hoechst (blue) and phalloidin (red) to identify the nucleus and actin cytoskeleton respectively. Cells were imaged using the GE IN Cell Analyzer 1000. Original magnification $\times$10.

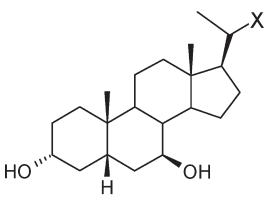

1l, X= $(CH_2)_2CN$
1m, X=CH_2CN
1n, X=CN
1o, X=$(CH_2)_3OH$
1p, X=CH_2COOH
1q, X=COOH
1r, X=$(CH_2)_2COOPh$
1s, X=$(CH_2)_2COOMe$

Figure 3. UDCA analogues **1l**−**s**.

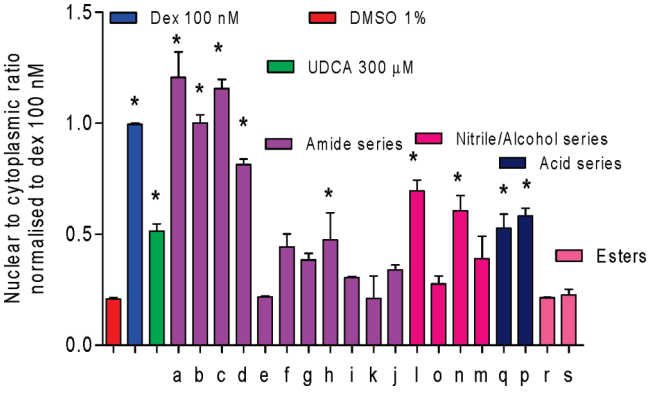

Figure 4. Analysis of GR translocation induced by UDCA derivatives. SKGT-4 cells were treated with DMSO 1%, Dex 100 nM as a positive control, UDCA 300 μM, or bile acid derivatives as indicated. All bile acid derivatives were initially screened at 300 μM. Cells were fixed, stained, and imaged as described, Original magnification, $\times$10. GR translocation was measured using the Investigator software package. Analysis was based on the ratio of the intensity of the GR within the nucleus and the intensity in the cytoplasm. Values are normalized to nuclear to cytoplasmic ratio of Dex 100 nM and are expressed as the mean $\pm$ SEM of two experiments performed in triplicate, * $p < 0.05$.

equal efficacy to UDCA with increased potency, 109.5, 123.5, and 109.0 μM, respectively. Extending the spacer by one carbon abolished activity (**1i**).

Table 1. EC_{50} Values for GR Translocation of UDCA (**1**) and Selected Modified Bile Acids [a]

compd	EC_{50} (μM, 95% CI) (% efficacy[b])
1	298.7 (151−432) (54)
1a	7.3 (1−14) (100)
1b	5.6 (2−10) (100)
1c	50.8 (29−88) (100)
1d	25.3 (17−31) (100)
1f	109.5 (60−149) (49)
1g	123.5 (57−191) (49)
1h	109.0 (42−168) (53)
1l	101.0 (44−168) (70)
1n	130.0 (25−181) (59)
1p	105.3 (54−161) (58)
1q	99.7 (51−154) (59)

[a] Compounds less active than UDCA are omitted. EC_{50} values for translocation after 4 h of treatment were determined from six point concentration-effect curves generated using nonlinear regression models Table 1. EC_{50} values for GR translocation of UDCA and selected modified bile acids. [b] Relative to Dex (100 nM).

Shortening the side chain but maintaining the acid functionality resulted in compounds with equal efficacy to UDCA but enhanced potency, norUDCA (**1p**) (EC_{50} of 105 μM) and bisnorUDCA (**1q**) (EC_{50} of 99.7 μM). The UDCA alcohol (**1o**) did not induce translocation, but conversion to the nitrile (**1l**) enhanced potency (EC_{50} of 100 μM, 70%). The bisnornitrile (**1n**) (EC_{50} of 130 μM, 59%) showed similar efficacy and potency to **1l** although the nornitrile (**1m**) did not induce translocation. UDCA methyl and benzyl esters (**1r**, **1s**) did not induce GR translocation.

Having shown that UDCA amides are moderately potent inducers of GR translocation, we investigated whether similar amide derivatives of DCA and CDCA could also induce translocation of the GR. The cyclopropyl and *N*-benzylpiperazine derivatives of DCA (**2**) (3α, 12α OH) and UDCA's

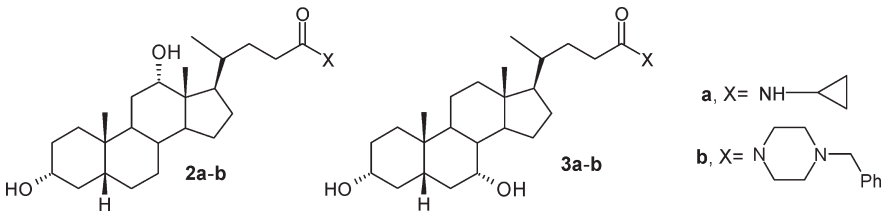

Figure 5. DCA and CDCA amides **2a**−**b**, **3a**−**b**.

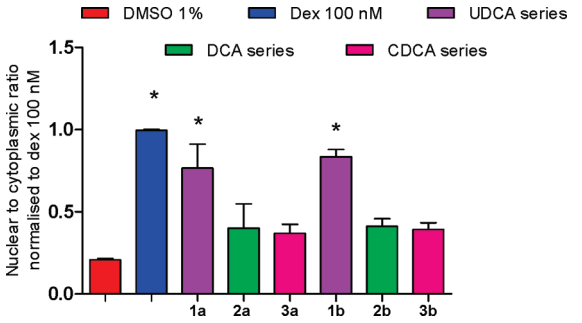

Figure 6. DCA and CDCA amides **2a**−**b**, **3a**−**b** do not induce GR translocation. SKGT-4 cells were (a) untreated or (b) treated with Dex 100 nM as a positive control, (c) cyclopropyl amide derivatives of UDCA, DCA, and CDCA (10 μM) (**1**−**3a**) or (d) benzylpiperidine derivatives of UDCA, DCA, and CDCA (10 μM) (**1**−**3b**) for 4 h and fixed, stained, and analyzed as described previously. Values are normalized to nuclear to cytoplasmic ratio of Dex (100 nM) and are expressed as the mean ± SEM of two experiments performed in triplicate, * $p < 0.05$.

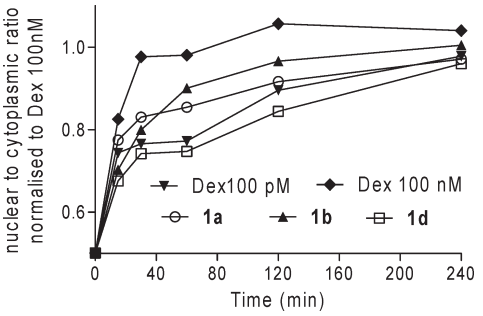

Figure 7. UDCA derivatives **1a**,**b**,**d** show similar translocation kinetics to Dex. SKGT-4 cells were treated with UDCA derivatives 100 μM or Dex at indicated concentration for 15, 30, 60, 120, or 240 min. Cells were fixed, stained, and analyzed for GR translocation as described previously. Values are normalized to nuclear to cytoplasmic ratio of Dex 100 nM and are expressed as the mean of two experiments performed in triplicate, $p < 0.05$ relative to DMSO 1%, for **1a** (120, 240 min), **1b** (60, 120, 240 min), **1d** (120, 240 min), Dex 100 pM (120, 240 min), Dex 100 nM (30, 60, 120, 240 min).

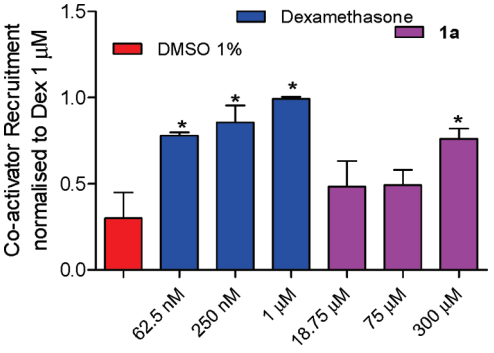

Figure 8. UDCA derivatives induce co-activator recruitment. A Lanthascreen TR-FRET GR coactivator assay was used to determine if the UDCA derivatives were capable of coactivator recruitment. Dex and **1a** were incubated at RT for 3 h with a GST-tagged GR-LBD and a mixture of the fluorescein labeled coactivator peptide and the terbium labeled anti-GST antibody. The TR-FRET ratio was calculated by dividing the emission signal at 520 nm by the emission signal at 495 nm. Values represent the mean ± SEM of three experiments performed in duplicate, normalized to positive control, Dex (1 μM).

epimer CDCA (**3**) (3α, 7α OH) were prepared, Figure 5. The DCA and CDCA amides (**2a**−**b**, **3a**−**b**) did not induce translocation at 10 μM (Figure 6). This indicates that the orientation of the OH groups on the steroid nucleus exerts a strong influence on the capacity of similar amides to induce GR translocation and it is consistent with a range of observations about the effects of UDCA compared with DCA and CDCA. The latter BAs promote apoptosis, whereas UDCA is anti-apoptotic, due in part to its ability to cause GR translocation.[45] The differing biological effects of DCA and CDCA relative to UDCA are attributed to the uninterrupted hydrophobic β-face of the former pair, although it is unclear whether this affects a macroscopic biophysical property or protein binding.

We examined the time course for GR translocation in the SKGT-4 cell line following treatment with analogues **1a**, **1b**, **1d**, and Dex to help characterize the kinetics of the effect. Following treatment with the UDCA amides produced a trend toward increased nuclear GR evident at 15 min; this achieved significance in 60 min in the case of **1b** and 120 min for **1a** and **1d**. The time course of a ligand-dependent protein event such as GR translocation is a function of the affinity of the ligand for the protein and ultimately ligand concentration. Therefore, Dex (100 nM) induced significant and maximum translocation of the GR at 30 min consistent with reported values, whereas at 100 pM, nuclear trafficking kinetics were more leisurely, with ratios reaching significance at 120 min, Figure 7. Overall, the time-course experiments indicated a direct effect on GR distribution rather than one downstream of protein synthesis. Furthermore, pretreatment of SKGT-4 cells with cycloheximide, an inhibitor of protein biosynthesis, did not affect **1a** induced GR translocation (Supporting Information (SI)). Cycloheximide did not induce translocation of the GR by itself. Hence **1a** induced GR translocation occurs independent of protein translation and in a similar time frame to Dex, albeit at a lower rate.

Even though UDCA and its active amides do not satisfy the classical GR pharmacophore, the most obvious explanation for their activity and time-course was ligand binding at the GR active site. However, selected active compounds (**1a**, **1p**, **1m**, **1h**) did not displace radiolabeled Dex in competition experiments at concentrations relevant to their ability to translocate. UDCA (10−50 μM) was also unable to displace Dex, consistent with previous studies.[39,41]

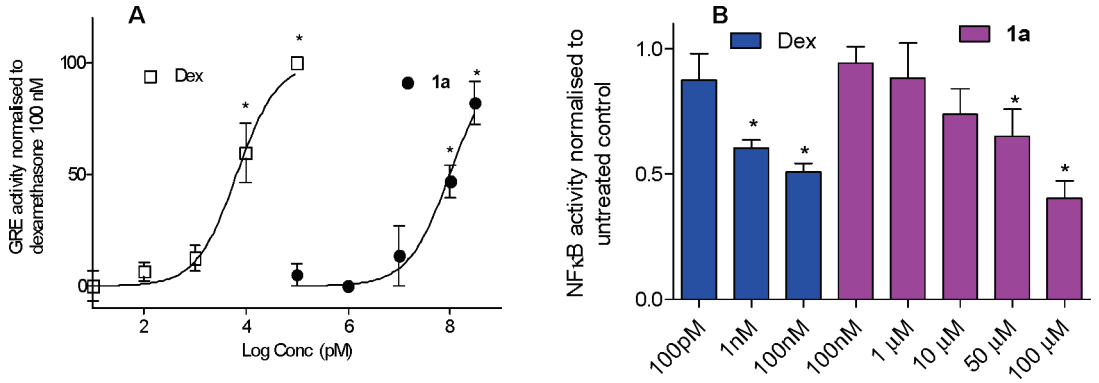

Figure 9. (A) UDCA derivatives transactivate the GR. SKGT-4 cells were transiently transfected with a mixture of an inducible glucocorticoid responsive firefly luciferase reporter and constitutively expressing Renilla construct (40:1). Cells were treated with increasing concentrations of Dex or **1a** for 16 h. Cells were then lysed and assayed for luciferase activity. Firefly luciferase activity was normalized to the internal vector control, renilla luciferase, to control for transfection efficiency. (B) UDCA derivatives decrease NFκB activity. HEK-293 cells were transiently transfected with an inducible NFκB responsive firefly luciferase reporter gene construct and a constitutively expressing β-galactosidase construct. After 24 h, the cells were treated with TNF-α 10 ng/μL alone or with TNF-α 10 ng/μL and varying concentrations of Dex or **1a**. After 16 h, the cells were lysed and the lysates assayed for firefly luciferase activity. Firefly luciferase activity was normalized to β-galactosidase activity to control for transfection efficiency. Values are expressed as the mean $\pm$ SEM of three experiments performed in duplicate, normalized to untreated control, * $p < 0.05$ relative to untreated control.

We next employed a time-resolved fluorescent energy transfer assay (TR-FRET) to try to detect an effect by UDCA or **1a** on GR coactivator recruitment which might indicate physical contact with the GR ensemble leading to conformational changes in the region of the LBD (Figure 8). **1a** (300 μM) increased the TR-FRET ratio to a significant extent, whereas UDCA (300 μM) did not. This result for UDCA is consistent with previous reports.[41] The DCA and CDCA compound **2a** and **3a** were unable to increase the TR-FRET ratio in the coactivator recruitment assay (data not shown).

Having demonstrated that the cyclopropylamide derivative (**1a**) was able to induce coactivator recruitment, our next step was to investigate whether treatment with **1a** could result in GR activation. We found that **1a** was able to induce GRE transactivation in a concentration dependent manner, reaching significance at 100 μM (Figure 9A). UDCA could only induce transactivation at 500 μM, but this did not follow a pharmacological trend (SI). The ability to attenuate NF-kB signaling is regarded as pivotal to the therapeutic actions of classical GCs. We therefore carried out a reporter assay to determine if **1a** could inhibit TNF-α induced NF-κB transcriptional activity in a HEK-293 cell line. We first showed that **1a** caused translocation of the GR in this cell line with similar potency and biochemical efficacy to the SKGT-4 cell line. Compound **1a** was capable of transrepression of NF-κB activity in a concentration dependent manner, $p < 0.05$ at 50 μM, 100 μM (Figure 9B).

The GR and MR are known to have widely overlapping ligand binding preferences and interrelated transcriptional activities, indeed, TUDCA causes translocation of both. However when MR expression was knocked down using siRNA, **1a** was still able to inhibit NF-κB transcriptional activity, whereas in the GR knock down condition, this effect was attenuated (SI). Furthermore, treatment with **1a** (50 μM) was not associated with nuclear translocation of the MR. Therefore, taking together the evidence of translocation exerted by **1a**, its ability to induce GRE transactivation and its GR dependent inhibition of NF-κB transcriptional activity, an agonist mode of action involving the GR is most likely. However, the potential involvement of other nuclear receptors merits further study.

UDCA has been shown to induce GR translocation in multiple cell models[41,42,48] at high concentrations (300 μM range). The mechanism by which UDCA induces GR translocation remains unknown despite extensive efforts over the past decade. Incubation of radiolabeled UDCA with the GR binding site expressed in a GR fusion protein yielded no specific binding of UDCA.[39] UDCA did not displace tritiated Dex from the GR binding site; furthermore, specific binding of tritiated UDCA to GR could not be detected in CHOpMTGR cells.[41] UDCA (10 and 50 μM) was unable to displace tritiated Dex in our competition binding experiment.

Despite this, UDCA requires the GR-LBD to induce GR nuclear translocation and for its subsequent biological effects.[41,45,49] Using a series of GR mutants, Miura et al showed that UDCA influences a broader region of the LBD than Dex. GR deletion mutants (1−765, 1−750, 1−740) could not be translocated by Dex but were by UDCA.[41] On the other hand, GR mutant 1−730 was unresponsive to UDCA. The specific carboxy terminal region of the LBD was identified as essential for translocation and UDCA's cytoprotective effect on TGFβ1 induced apoptosis.[49] This mutant lacks Tyr735 of the steroid binding pocket, which is necessary for hydrophobic contact between ligands and the GR.[50]

The ability of UDCA to induce GR activation downstream of translocation remains a matter of debate as studies are widely conflicted over its ability to activate GREs.[39,41,42,49] Previous investigators failed to show an interaction between UDCA and the coactivator transcription intermediary factor-2.[41] Other studies have shown that UDCA can have an additive effect with GCs in inducing gene expression. For example, UDCA increased Dex induced mRNA levels of tyrosine aminotransferase (TAT), a hepatocyte-specific marker of GC action.[51] Others have shown that combining UDCA and Dex can increase the expression of the bicarbonate carrier, AE2, altered expression of which is associated with PBC. It has been suggested that certain genes contain only half of a GRE site referred to as GRE cores. Binding of GR to GRE core sites may require further assistance in addition to the interaction with GCs which UDCA may provide.[52]

Similar to UDCA, there is not a defined mechanism for GR translocation induced by its more active amides. The most

potent GR translocator **1a** was unable to displace tritiated Dex in a competition binding experiment at similar concentration to its EC_{50} for translocation. Previous authors have suggested that UDCA may interact with the cell membrane and set up a series of cytoplasmic events through secondary signals, one of which may be GR activation.[41,45] Such an explanation cannot be ruled out for the derivatives although GR translocation by the amides displayed a similar time profile to Dex. Furthermore **1a** was able to induce coactivator recruitment in a cell free system. Recruitment of steroid receptor coactivator 1−4 (SRC1−4) by **1a** indicates that it can induce the necessary conformational change in the GR-LBD. This recruitment was specific to the UDCA core nucleus as the corresponding derivatives of DCA and CDCA did not cause coactivator recruitment.

Conclusion

We have discovered amido derivatives of UDCA that causes GR translocation in the low micromolar range in SKGT-4 cells. These compounds do no bind at the classical GC binding locus, but they affect coactivator recruitment and cause transactivation at high concentration. The most potent compound decreased NF-κB activity in a HEK-293 line with moderate potency.

Taken together, the data suggests that UDCA amides bind to the LBD but at a different site to the classical pocket, binding to which accounts for the actions of established GR modulators, including dissociated steroids which separate transactivation from transrepression.[53−56] UDCA has well established but poorly understood effects on cellular function that appear to be mediated at least in part by the GR. The amido analogues reported herein amplify this activity by about 100-fold. They hold potential in therapeutic applications and in exploring ongoing puzzles associated with the actions of UDCA.

Experimental Section

Chemistry. Uncorrected melting points were obtained using a Stuart melting point SMP11 melting point apparatus. IR spectra were obtained using a Perkin-Elmer 205 FT Infrared Paragon 1000 spectrometer. Band positions are given in cm^{-1}. Solid samples were obtained by KBr disk; oils were analyzed as neat films on NaCl plates. ^1H and ^{13}C spectra were recorded at 27 °C on a Bruker Advance II 600 MHz spectrometer (600.13 MHz ^1H, 150.91 MHz ^{13}C) and Bruker DPX 400 MHz FT NMR spectrometer (400.13 MHz ^1H, 100.16 MHz ^{13}C) in either $CDCl_3$ or CD_3OD (tetramethylsilane as internal standard). For $CDCl_3$, ^1H NMR spectra were assigned relative to the TMS peak at 0.00 δ and ^{13}C NMR spectra were assigned relative to the middle $CDCl_3$ triplet at 77.00 ppm. For CD_3OD, ^1H and ^{13}C NMR spectra were assigned relative to the center peaks of the CD_3OD multiplets at 3.30 δ and 49.00 ppm, respectively. High-resolution mass spectrometry (HRMS) was performed on a Micromass mass spectrophotometer (EI mode) at the Department of Chemistry, Trinity College. High-performance liquid chromatography (HPLC) was performed on a reversed phase 250 mm × 4.6 mm Waters Spherisorb ODS-2, 5 μm column using a Waters Alliance 2695 chromatograph equipped with an autosampler, column oven, and dual wavelength detector. The flow rate was 1 mL/min, with a mobile phase consisting of 40% phosphate buffer pH 2.5 and 60% acetonitrile at time 0 and grading to 85% acetonitrile at 4 min. Injection volume was 20 μL and areas determined at 254 nm. The isocratic HPLC method was aqueous phosphate buffer solution pH 2.5 40% and acetonitrile 60%. Flow rate was 1 mL/min. Flash chromatography was performed on Merck Kieselgel 60 particle size 0.040−0.063 mm. Thin layer chromatography (TLC) was performed on silica gel Merck F-254 plates. Compounds were visually detected by absorbance at 254 nm and/or vanillin staining. All test compounds were ≥95% purity by HPLC.

24-Cyclopropyl-3α,7β-dihydroxy-5β-cholanamide (1a). 3α,7β-Diformyloxy-5β-cholan-24-oic acid (1.0 g, 2 mmol) was dissolved in thionyl chloride (5 mL) and refluxed at 90 °C for 2 h. After 1 h, the reaction was cooled to room temperature and the thionyl chloride was removed in vacuo to leave a sticky solid which was the acid chloride. This was dissolved in dry DCM (10 mL) and cyclopropylamine (131 μL, 1.9 mmol) and triethylamine (244 μL, 1.9 mmol) were added on ice. The reaction mixture was allowed to warm to room temperature and stirred monitoring for disappearance of the starting material by TLC. After 24 h, the solvent was removed in vacuo. The residue was dissolved in ethyl acetate (20 mL) and washed with hydrochloric acid (HCl) (3 × 20 mL) for removal of unreacted amines, water (2 × 20 mL), and brine solution (2 × 20 mL). The organic layer was dried and evaporation of solvent gave the cyclopropylamide after chromatographic elution (hexane:ethyl acetate 1:1). Sodium (0.1 g) was added to HPLC grade methanol (MeOH) (10 mL) to form an excess of sodium methoxide. The formyl cyclopropylamide (0.5 g, 1 mmol) was added to this solution and refluxed for 2 h. After 2 h, the reaction was cooled to room temperature and added to water (100 mL). The amide was extracted with ethyl acetate. The organic layer was then washed with water (3 × 20 mL) and dried ($MgSO_4$). The solvent was removed in vacuo and after chromatographic elution with ethyl acetate afforded a white solid (0.4 g, 92%). ^1H NMR δ (CD_3OD): 0.49 (2-H, m), 0.65 (3-H, s), 0.92 (3-H, d, J = 6.52 Hz), 0.97 (3-H, s), 2.75 (1-H, m), 3.61 (2-H, m), 5.32 (1-H, br). ^{13}C NMR ppm (CD_3OD): 8.4, 12.4, 18.8, 22.4, 24.0, 25.2, 25.5, 28.0, 29.8, 31.1, 35.3, 36.5, 36.9, 38.1, 38.8, 40.9, 41.7, 44.1, 44.6, 44.9, 56.5, 57.8, 71.1, 175.2. HRMS: found $(M - Na)^+$ = 454.3297. Melting point 124 °C

24-*N*-Benzylpiperazine-3α,7β-dihydroxy-5β-cholanamide (1b). ^1H NMR δ (CD_3OD): 0.70 (3-H, s, 18-CH_3), 0.95 (6-H, m), 3.41−3.60 (8-H, m), 3.52 (2-H, m). ^{13}C NMR ppm (CD_3OD): 12.9, 19.0, 22.5, 24.0, 28.0, 29.8, 31.1, 32.2, 32.5, 35.1, 36.1, 36.8, 38.1, 38.9, 39.2, 40.9, 41.7, 44.2, 44.7, 44.9, 45.3, 56.6, 57.8, 71.1, 80.3, 130.2, 175.5. HRMS: found $(M - Na)^+$ = 573.4097. Melting point 116 °C.

Biochemistry. Chemicals. Dex, UDCA, and all reagents for chemical synthesis were obtained from Sigma-Aldrich Chemical Co. (St. Louis, MO, USA). Lipofectamine was purchased from Invitrogen (Carlsbad, CA, USA). TNF-α was purchased from R&D Systems and reconstituted with sterile PBS at 100 μg/mL. Cycloheximide (Calbiochem, Merck Chemicals Ltd. Nottingham, UK) was reconstituted with ethanol at a concentration of 20 mg/mL. *Escherichia coli* lipopolysaccharide was obtained from Alexis Biochemicals (San Diego, CA, USA).

Dex was dissolved in DMSO to give a 10 mM stock solution, and all other bile acids and bile acid derivatives were maintained as 200 mM stock solutions in DMSO. The compounds were diluted to the required concentrations with medium with 1% DMSO in order to maintain solubility.

A Smartpool of predesigned siRNA oligos (ON-TARGET *plus* siRNA reagents) targeting the glucocorticoid receptor (siGR), mineralocorticoid receptor (siMR), scrambled control siRNA (siScr), and siRNA transfection reagent were purchased from Dharmacon (Lafayette, CO, USA).

Cell Culture. The SKGT4 cell line, derived from a well-differentiated adenocarcinoma arising in Barrett's epithelium of the distal esophagus, was generously provided by Dr. David Schrump (Bethesda, MA).[57] Cells were maintained in RPMI 1640 medium supplemented with 10% fetal bovine serum and 4 mM L-glutamine (GIBCO-BRL, Grand Island, NY) HEK-293 cells, an adherent human embryonic kidney cell line, were grown in Dulbecco's Modified Eagle's Medium (DMEM, GIBCO, Invitrogen Ltd., Paisley, UK) supplemented with 10%

heat-inactivated FBS. Cultures were maintained at 37 °C in a humidified atmosphere containing 5% CO_2.

GR Translocation Assay. Cells were plated into 96-well plates at a concentration of 6×10^4 cells/mL (100 μL volume). Cells were serum starved for 12 h prior to bile acid treatment. After 48 h, cells were treated with bile acid derivatives in supplement free medium at the required concentration for the indicated time points. Control wells were left untreated or treated with 1% DMSO as a vehicle control or Dex 100 nM as positive control. After the appropriate treatment time, cells were fixed with 4% paraformaldehyde/phosphate buffered saline (PBS) then permeabilized with 0.1% (v/v) Triton X-100/PBS followed by blocking with 3% bovine serum albumin in PBS. Cells were incubated with purified mouse antiglucocorticoid receptor antibody (BD Transduction Laboratories) then incubated with AlexaFluor-488-conjugated secondary antibody (Invitrogen, Carlsbad, CA, USA). Images were acquired using the GE IN cell analyzer 1000, original magnification ×10. Four fields of view per well were acquired using a 10× objective, with up to 2000 cells imaged per treatment group, for $n = 3$ experiments.

Quantification of GR Translocation Using High Content Analysis. The GE IN cell analyzer 1000 is a microscope based screening platform capable of large scale objective analysis of fluorescently labeled cells using automated image acquisition, data management, and multiparametric analysis. SKGT-4s were stained for GR as outlined above. Nuclear to cytoplasmic ratio was measured using the Investigator software package (GE Healthcare, Piscataway, NJ, USA). The analysis was based on the ratio of the intensities of GR within the nucleus and cytoplasm. The multitarget analysis algorithm was optimized to detect GR within the nucleus and the cytoplasm using vehicle only treated cells as negative control and Dex treated cells as positive control. Hoechst staining enabled identification of the nucleus. The nuclear to cytoplasmic ratios were determined by calculating (nuclear Intensity of GR − background intensity)/(cytoplasmic intensity of GR − background intensity). Values represent the mean ± SEM of three experiments performed in triplicate. EC_{50} values were estimated from concentration−effect curves generated using nonlinear regression models in GraphPad Prism5.

GRE Assay. SKGT-4 cells were transiently transfected with a mixture of an inducible glucocorticoid responsive firefly luciferase reporter and constitutively expressing renilla construct (40:1) (SABiosciences Corporation, Executive Way, Frederick, MD, USA). A reverse transfection procedure was optimized using fugene HD as a transfection reagent at a ratio of 4:1 (Fugene HD:DNA). DNA and Fugene HD were diluted in OptiMem, and this mixture was added to 96-well plates to give 100 ng DNA per well. SKGT-4 cells at a density of 7×10^4 cells/mL (100 μL) were added to this mixture. After 24 h, the cells were treated with varying concentrations of Dex or **1a** for 16 h. After 16 h, the cells were lysed using passive lysis buffer 50 μL (Promega Corporation, Madison, WI, USA) and incubated at room temperature for 15 min. The lysates were then assayed for firefly and renilla luciferase activity (Promega Dual-Luciferase Reporter Assay System) using a Victor Perkin-Elmer luminometer. Values represent the mean ± SEM of three experiments performed in duplicate, normalized to Dex 100 nM as positive control.

Time-Resolved Fluorescence Resonance Energy Transfer Assay. TR-FRET is based on the principle that when a suitable pair of fluorophores is brought within close proximity of one another, excitation of the first fluorophore results in energy transfer to the second fluorophore. This can be detected by an increase in the fluorescence emission of the acceptor molecule and a decrease in the fluorescence emission of the donor molecule. We used a Lanthascreen TR-FRET glucocorticoid receptor coactivator assay kit (Invitrogen, Carlsbad, CA, USA), which provides a human GR-LBD tagged with a glutathione-*S*-transferase (GST), a terbium-labeled anti-GST antibod,y and a fluorescein labeled SRC1−4 peptide. Binding of agonist to the nuclear receptor causes a conformational change in the LBD of the GR, which results in recruitment of the coactivator peptide. When the terbium label on the anti-GST antibody is excited at 340 nm, energy is transferred to the fluorescein label on the coactivator peptide and detected as emission at 520 nm. The GR-LBD was added to the indicated concentration of Dex, **1a**, **2a**, and **3a** in a 384-well black assay plates (Corning BV Life Sciences, Fogostraat, Amsterdam, The Netherlands) followed by addition of a mixture of the fluorescein labeled coactivator peptide and the terbium labeled anti-GST antibody. The plates were incubated at room temperature for 3 h and then measured for TR-FRET activity using the LanthaScreen optic filter module on the BMG pherastar (Imgen Technologies, VA, USA). The TR-FRET ratio was calculated by dividing the emission signal at 520 nm by the emission signal at 495 nm. Values represent the mean ± SEM of three experiments performed in duplicate, normalized to positive control, Dex 1 μM.

NF-κB Assay. HEK-293 cells were transiently cotransfected with an inducible NF-κB responsive construct, which contains 3 κB elements upstream of a minimal conalbumin promoter linked to the firefly luciferase gene[58] and a constitutively expressing β-galactosidase construct (Clontech, Saint-Germain-en-Laye, France) as an internal control to monitor for transfection efficiency (ratio of 4:1). A reverse transfection procedure was carried out using lipofectamine as a transfection reagent at a ratio of 3:2 (lipofectamine:DNA). DNA and lipofectamine were diluted in OptiMem, and this mixture was added to 48-well plates to give 500 ng of DNA per well. HEK-293 cells at a density of 7×10^5 cells/mL (200 μL) were added to this mixture. After 24 h, the cells were treated with TNF-α 10 ng/μL alone or with TNF-α 10 ng/μL and varying concentrations of Dex or CPA (**1a**) for 16 h. After 16 h, the cells were lysed with Promega lysis buffer (50 μL) and the lysates assayed for firefly luciferase activity (Promega Corporation, Madison, WI, USA). The lysates were then assayed for β-galactosidase activity using *o*-nitrophenyl-β-D-galactopyranoside as a substrate following methods described by Sambrook et al.[59] Values are expressed as the mean ± SEM of three experiments performed in duplicate, normalized to untreated control, * $p < 0.05$ relative to untreated control.

Radioligand Binding Assay. Human HeLa S3 cells enriched with GRs were used in HEPES/RPMI-1640 buffer pH 7.2. Cells (3×10^6) were incubated with 3 nM [^{3}H] Dex for 120 min at 25 °C. Nonspecific binding was estimated in the presence of Dex (10 μM). Cells were filtered and washed, and the filters were then counted to determine [^{3}H] Dex specifically bound. UDCA derivatives were screened at 10 μM and UDCA at 10 and 50 μM.

Statistical Analysis. Statistical comparison between groups was carried out using one way ANOVA with Dunnett's posthoc correction. Data are graphically represented as the mean ± standard error of the mean (SEM). All data were analyzed using GraphPad Prism5.

Acknowledgment. We thank Dr. John O'Brien and Dr. Manuel Reuther for NMR spectroscopy, Dr. Martin Feeney and Dr. Dilip Rai for HRMS data, Dr. Sinead Smith for assistance with plasmids, and Ray Keaveney for HPLC work. This work was supported by the Health Research Board [TRA/2007/11, Esophageal Cancer−Toward New Therapies] and the Embark Initiative (IRCSET Award to Sharma, 2006).

Supporting Information Available: Characterization and purity data, biochemistry figures. This material is available free of charge via the Internet at http://pubs.acs.org.

References

(1) Renaud, J. P.; Moras, D. Structural studies on nuclear receptors. *Cell. Mol. Life Sci.* **2000**, *57*, 1748–1769.
(2) Stahn, C.; Lowenberg, M.; Hommes, D. W.; Buttgereit, F. Molecular mechanisms of glucocorticoid action and selective glucocorticoid receptor agonists. *Mol. Cell. Endocrinol.* **2007**, *275*, 71–78.
(3) Banciu, M.; Schiffelers, R. M.; Metselaar, J. M.; Storm, G. Utility of targeted glucocorticoids in cancer therapy. *J. Liposome Res.* **2008**, *18*, 47–57.
(4) Heitzer, M. D.; Wolf, I. M.; Sanchez, E. R.; Witchel, S. F.; DeFranco, D. B. Glucocorticoid receptor physiology. *Rev. Endocr. Metab. Disord.* **2007**, *8*, 321–330.
(5) Necela, B. M.; Cidlowski, J. A. Mechanisms of glucocorticoid receptor action in noninflammatory and inflammatory cells. *Proc. Am. Thorac. Soc.* **2004**, *1*, 239–246.
(6) Starr, D. B.; Matsui, W.; Thomas, J. R.; Yamamoto, K. R. Intracellular receptors use a common mechanism to interpret signaling information at response elements. *Genes Dev.* **1996**, *10*, 1271–1283.
(7) Smirnov, A. N. Nuclear receptors: nomenclature, ligands, mechanisms of their effects on gene expression. *Biochemistry* (*Moscow*) **2002**, *67*, 957–977.
(8) Jenkins, B. D.; Pullen, C. B.; Darimont, B. D. Novel glucocorticoid receptor coactivator effector mechanisms. *Trends Endocrinol. Metab.* **2001**, *12*, 122–126.
(9) Deroo, B. J.; Archer, T. K. Glucocorticoid receptor-mediated chromatin remodeling in vivo. *Oncogene* **2001**, *20*, 3039–3046.
(10) Morrison, N.; Eisman, J. Role of the negative glucocorticoid regulatory element in glucocorticoid repression of the human osteocalcin promoter. *J. Bone Miner. Res.* **1993**, *8*, 969–975.
(11) Sakai, D. D.; Helms, S.; Carlstedt-Duke, J.; Gustafsson, J. A.; Rottman, F. M.; Yamamoto, K. R. Hormone-mediated repression: a negative glucocorticoid response element from the bovine prolactin gene. *Genes Dev.* **1988**, *2*, 1144–1154.
(12) Yudt, M. R.; Cidlowski, J. A. The glucocorticoid receptor: coding a diversity of proteins and responses through a single gene. *Mol. Endocrinol.* **2002**, *16*, 1719–1726.
(13) Zanchi, N. E.; Filho, M. A.; Felitti, V.; Nicastro, H.; Lorenzeti, F. M.; Lancha, A. H., Jr. Glucocorticoids: extensive physiological actions modulated through multiple mechanisms of gene regulation. *J. Cell. Physiol.* **2010**, *224*, 311–315.
(14) Rosen, J.; Miner, J. N. The search for safer glucocorticoid receptor ligands. *Endocr. Rev.* **2005**, *26*, 452–464.
(15) Vayssiere, B. M.; Dupont, S.; Choquart, A.; Petit, F.; Garcia, T.; Marchandeau, C.; Gronemeyer, H.; Resche-Rigon, M. Synthetic glucocorticoids that dissociate transactivation and AP-1 transrepression exhibit antiinflammatory activity in vivo. *Mol. Endocrinol.* **1997**, *11*, 1245–1255.
(16) Belvisi, M. G.; Wicks, S. L.; Battram, C. H.; Bottoms, S. E.; Redford, J. E.; Woodman, P.; Brown, T. J.; Webber, S. E.; Foster, M. L. Therapeutic benefit of a dissociated glucocorticoid and the relevance of in vitro separation of transrepression from transactivation activity. *J. Immunol.* **2001**, *166*, 1975–1982.
(17) Xiao, H. Y.; Wu, D. R.; Malley, M. F.; Gougoutas, J. Z.; Habte, S. F.; Cunningham, M. D.; Somerville, J. E.; Dodd, J. H.; Barrish, J. C.; Nadler, S. G.; Dhar, T. G. Novel synthesis of the hexahydroimidazo[1,5*b*]isoquinoline scaffold: application to the synthesis of glucocorticoid receptor modulators. *J. Med. Chem.* **2010**, *53*, 1270–1280.
(18) Schoch, G. A.; D'Arcy, B.; Stihle, M.; Burger, D.; Bar, D.; Benz, J.; Thoma, R.; Ruf, A. Molecular switch in the glucocorticoid receptor: active and passive antagonist conformations. *J. Mol. Biol.* **2010**, *395*, 568–577.
(19) De Bosscher, K. Selective Glucocorticoid Receptor modulators. *J Steroid Biochem Mol. Biol.* **2009**, *120*, 96–104.
(20) Heathcote, E. J. Management of primary biliary cirrhosis. The American Association for the Study of Liver Diseases practice guidelines. *Hepatology* **2000**, *31*, 1005–1013.
(21) Azzaroli, F.; Mehal, W.; Soroka, C. J.; Wang, L.; Lee, J.; Crispe, N.; Boyer, J. L. Ursodeoxycholic acid diminishes Fas-ligand-induced apoptosis in mouse hepatocytes. *Hepatology* **2002**, *36*, 49–54.
(22) Amaral, J. D.; Castro, R. E.; Steer, C. J.; Rodrigues, C. M. p53 and the regulation of hepatocyte apoptosis: implications for disease pathogenesis. *Trends Mol. Med.* **2009**, *15*, 531–541.
(23) Rodrigues, C. M.; Ma, X.; Linehan-Stieers, C.; Fan, G.; Kren, B. T.; Steer, C. J. Ursodeoxycholic acid prevents cytochrome c release in apoptosis by inhibiting mitochondrial membrane depolarization and channel formation. *Cell Death Differ.* **1999**, *6*, 842–854.
(24) Fimognari, C.; Lenzi, M.; Cantelli-Forti, G.; Hrelia, P. Apoptosis and modulation of cell cycle control by bile acids in human leukemia T cells. *Ann. N.Y. Acad. Sci.* **2009**, *1171*, 264–269.
(25) Keene, C. D.; Rodrigues, C. M.; Eich, T.; Chhabra, M. S.; Steer, C. J.; Low, W. C. Tauroursodeoxycholic acid, a bile acid, is neuroprotective in a transgenic animal model of Huntington's disease. *Proc. Natl. Acad. Sci. U.S.A* **2002**, *99*, 10671–10676.
(26) Keene, C. D.; Rodrigues, C. M.; Eich, T.; Linehan-Stieers, C.; Abt, A.; Kren, B. T.; Steer, C. J.; Low, W. C. A bile acid protects against motor and cognitive deficits and reduces striatal degeneration in the 3-nitropropionic acid model of Huntington's disease. *Exp. Neurol.* **2001**, *171*, 351–360.
(27) Lukivskaya, O.; Zavodnik, L.; Knas, M.; Buko, V. Antioxidant mechanism of hepatoprotection by ursodeoxycholic acid in experimental alcoholic steatohepatitis. *Adv. Med. Sci.* **2006**, *51*, 54–59.
(28) Alberts, D. S.; Martinez, M. E.; Hess, L. M.; Einspahr, J. G.; Green, S. B.; Bhattacharyya, A. K.; Guillen, J.; Krutzsch, M.; Batta, A. K.; Salen, G.; Fales, L.; Koonce, K.; Parish, D.; Clouser, M.; Roe, D.; Lance, P. Phase III trial of ursodeoxycholic acid to prevent colorectal adenoma recurrence. *J. Natl. Cancer Inst.* **2005**, *97*, 846–853.
(29) Shah, S. A.; Looby, E.; Volkov, Y.; Long, A.; Kelleher, D. Ursodeoxycholic acid inhibits translocation of protein kinase C in human colonic cancer cell lines. *Eur. J. Cancer* **2005**, *41*, 2160–2169.
(30) Khare, S.; Mustafi, R.; Cerda, S.; Yuan, W.; Jagadeeswaran, S.; Dougherty, U.; Tretiakova, M.; Samarel, A.; Cohen, G.; Wang, J.; Moore, C.; Wali, R.; Holgren, C.; Joseph, L.; Fichera, A.; Li, Y. C.; Bissonnette, M. Ursodeoxycholic acid suppresses Cox-2 expression in colon cancer: roles of Ras, p38, and CCAAT/enhancer-binding protein. *Nutr. Cancer* **2008**, *60*, 389–400.
(31) Shah, S. A.; Volkov, Y.; Arfin, Q.; Abdel-Latif, M. M.; Kelleher, D. Ursodeoxycholic acid inhibits interleukin 1 beta [corrected] and deoxycholic acid-induced activation of NF-kappaB and AP-1 in human colon cancer cells. *Int. J. Cancer* **2006**, *118*, 532–539.
(32) Poupon, R. E.; Balkau, B.; Eschwege, E.; Poupon, R. A multicenter, controlled trial of ursodiol for the treatment of primary biliary cirrhosis. UDCA-PBC Study Group. *N Engl. J. Med.* **1991**, *324*, 1548–1554.
(33) Miyaguchi, S.; Mori, M. Ursodeoxycholic acid (UDCA) suppresses liver interleukin 2 mRNA in the cholangitis model. *Hepatogastroenterology* **2005**, *52*, 596–602.
(34) Saeki, R.; Ogino, H.; Kaneko, S.; Unoura, M.; Kobayashi, K. Effects of chenodeoxycholic and ursodeoxycholic acids on interferon-gamma production by peripheral blood mononuclear cells from patients with primary biliary cirrhosis. *J. Gastroenterol.* **1995**, *30*, 739–744.
(35) Calmus, Y.; Gane, P.; Rouger, P.; Poupon, R. Hepatic expression of class I and class II major histocompatibility complex molecules in primary biliary cirrhosis: effect of ursodeoxycholic acid. *Hepatology* **1990**, *11*, 12–15.
(36) Terasaki, S.; Nakanuma, Y.; Ogino, H.; Unoura, M.; Kobayashi, K. Hepatocellular and biliary expression of HLA antigens in primary biliary cirrhosis before and after ursodeoxycholic acid therapy. *Am. J. Gastroenterol.* **1991**, *86*, 1194–1199.
(37) Nishigaki, Y.; Ohnishi, H.; Moriwaki, H.; Muto, Y. Ursodeoxycholic acid corrects defective natural killer activity by inhibiting prostaglandin E2 production in primary biliary cirrhosis. *Dig. Dis. Sci.* **1996**, *41*, 1487–1493.
(38) Ikegami, T.; Matsuzaki, Y.; Fukushima, S.; Shoda, J.; Olivier, J. L.; Bouscarel, B.; Tanaka, N. Suppressive effect of ursodeoxycholic acid on type IIA phospholipase A2 expression in HepG2 cells. *Hepatology* **2005**, *41*, 896–905.
(39) Weitzel, C.; Stark, D.; Kullmann, F.; Scholmerich, J.; Holstege, A.; Falk, W. Ursodeoxycholic acid induced activation of the glucocorticoid receptor in primary rat hepatocytes. *Eur. J. Gastroenterol. Hepatol.* **2005**, *17*, 169–177.
(40) Tanaka, H.; Makino, I. Ursodeoxycholic acid-dependent activation of the glucocorticoid receptor. *Biochem. Biophys. Res. Commun.* **1992**, *188*, 942–948.
(41) Miura, T.; Ouchida, R.; Yoshikawa, N.; Okamoto, K.; Makino, Y.; Nakamura, T.; Morimoto, C.; Makino, I.; Tanaka, H. Functional modulation of the glucocorticoid receptor and suppression of NF-kappaB-dependent transcription by ursodeoxycholic acid. *J. Biol. Chem.* **2001**, *276*, 47371–47378.
(42) Tanaka, H.; Makino, Y.; Miura, T.; Hirano, F.; Okamoto, K.; Komura, K.; Sato, Y.; Makino, I. Ligand-independent activation of the glucocorticoid receptor by ursodeoxycholic acid. Repression of IFN-gamma-induced MHC class II gene expression via a glucocorticoid receptor-dependent pathway. *J. Immunol.* **1996**, *156*, 1601–1608.
(43) Abdel-Latif, M. M.; Duggan, S.; Reynolds, J. V.; Kelleher, D. Inflammation and esophageal carcinogenesis. *Curr. Opin. Pharmacol.* **2009**, *9*, 396–404.
(44) Sola, S.; Amaral, J. D.; Borralho, P. M.; Ramalho, R. M.; Castro, R. E.; Aranha, M. M.; Steer, C. J.; Rodrigues, C. M. Functional

modulation of nuclear steroid receptors by tauroursodeoxycholic acid reduces amyloid beta-peptide-induced apoptosis. *Mol. Endocrinol.* **2006**, *20*, 2292–2303.
(45) Sola, S.; Castro, R. E.; Kren, B. T.; Steer, C. J.; Rodrigues, C. M. Modulation of nuclear steroid receptors by ursodeoxycholic acid inhibits TGF-beta1-induced E2F-1/p53-mediated apoptosis of rat hepatocytes. *Biochemistry* **2004**, *43*, 8429–8438.
(46) Schteingart, C. D.; Hofmann, A. F. Synthesis of 24-nor-5 beta-cholan-23-oic acid derivatives: a convenient and efficient one-carbon degradation of the side chain of natural bile acids. *J. Lipid Res.* **1988**, *29*, 1387–1395.
(47) Liliang, H.; Hua, Z.; Xiaoping, X.; Chunchun, Z.; Yu-Mei, S. Synthesis and charcterisation of organometallic rhenium (I) and technetium (I) bile acid complexes. *J. Organomet. Chem.* **2009**, *694*, 3247–3253.
(48) Angulo, P.; Lindor, K. D. Management of primary biliary cirrhosis and autoimmune cholangitis. *Clin. Liver Dis.* **1998**, *2*, 333−351, ix.
(49) Sola, S.; Amaral, J. D.; Castro, R. E.; Ramalho, R. M.; Borralho, P. M.; Kren, B. T.; Tanaka, H.; Steer, C. J.; Rodrigues, C. M. Nuclear translocation of UDCA by the glucocorticoid receptor is required to reduce TGF-beta1-induced apoptosis in rat hepatocytes. *Hepatology* **2005**, *42*, 925–934.
(50) Stevens, A.; Garside, H.; Berry, A.; Waters, C.; White, A.; Ray, D. Dissociation of steroid receptor coactivator 1 and nuclear receptor corepressor recruitment to the human glucocorticoid receptor by modification of the ligand−receptor interface: the role of tyrosine 735. *Mol. Endocrinol.* **2003**, *17*, 845–859.
(51) Mitsuyoshi, H.; Nakashima, T.; Inaba, K.; Ishikawa, H.; Nakajima, Y.; Sakamoto, Y.; Matsumoto, M.; Okanoue, T.; Kashima, K. Ursodeoxycholic acid enhances glucocorticoid-induced tyrosine aminotransferase-gene expression in cultured rat hepatocytes. *Biochem. Biophys. Res. Commun.* **1997**, *240*, 732–736.
(52) Arenas, F.; Hervias, I.; Uriz, M.; Joplin, R.; Prieto, J.; Medina, J. F. Combination of ursodeoxycholic acid and glucocorticoids upregulates the AE2 alternate promoter in human liver cells. *J. Clin. Invest.* **2008**, *118*, 695–709.
(53) Newton, R.; Holden, N. S. Separating transrepression and transactivation: a distressing divorce for the glucocorticoid receptor? *Mol. Pharmacol.* **2007**, *72*, 799–809.
(54) Belvisi, M. G.; Brown, T. J.; Wicks, S.; Foster, M. L. New Glucocorticosteroids with an improved therapeutic ratio? *Pulm. Pharmacol. Ther.* **2001**, *14*, 221–227.
(55) Regan, J.; Lee, T. W.; Zindell, R. M.; Bekkali, Y.; Bentzien, J.; Gilmore, T.; Hammach, A.; Kirrane, T. M.; Kukulka, A. J.; Kuzmich, D.; Nelson, R. M.; Proudfoot, J. R.; Ralph, M.; Pelletier, J.; Souza, D.; Zuvela-Jelaska, L.; Nabozny, G.; Thomson, D. S. Quinol-4-ones as steroid A-ring mimetics in nonsteroidal dissociated glucocorticoid agonists. *J. Med. Chem.* **2006**, *49*, 7887–7896.
(56) Barker, M.; Clackers, M.; Copley, R.; Demaine, D. A.; Humphreys, D.; Inglis, G. G.; Johnston, M. J.; Jones, H. T.; Haase, M. V.; House, D.; Loiseau, R.; Nisbet, L.; Pacquet, F.; Skone, P. A.; Shanahan, S. E.; Tape, D.; Vinader, V. M.; Washington, M.; Uings, I.; Upton, R.; McLay, I. M.; Macdonald, S. J. Dissociated nonsteroidal glucocorticoid receptor modulators; discovery of the agonist trigger in a tetrahydronaphthalene-benzoxazine series. *J. Med. Chem.* **2006**, *49*, 4216–4231.
(57) Altorki, N.; Schwartz, G. K.; Blundell, M.; Davis, B. M.; Kelsen, D. P.; Albino, A. P. Characterization of cell lines established from human gastric−esophageal adenocarcinomas. Biologic phenotype and invasion potential. *Cancer* **1993**, *72*, 649–657.
(58) Arenzana-Seisdedos, F.; Fernandez, B.; Dominguez, I.; Jacque, J. M.; Thomas, D.; Diaz-Meco, M. T.; Moscat, J.; Virelizier, J. L. Phosphatidylcholine hydrolysis activates NF-kappa B and increases human immunodeficiency virus replication in human monocytes and T lymphocytes. *J. Virol.* **1993**, *67*, 6596–6604.
(59) Sambrook, J.; Russel, D. W. *Molecular Cloning: A Laboratory Manual*, 3rd ed.; Cold Spring Harbour Laboratory Press: New York, 2001; Vol. 2.